A New Set of Indicators to Evaluate the Bioclimatic Performance of Air Conditioned Buildings in a Hot and Humid Climate

Abdou Idris Omar, Damien David, Joseph Virgone, Abdoulkader Ibrahim Idriss, Étienne Vergnault

A New Set of Indicators to Evaluate the Bioclimatic Performance of Air Conditioned Buildings in a Hot and Humid Climate

Abdou Idris Omar[1,2], Damien David[2], Etienne Vergnault[2], Joseph Virgone[2], Abdoulkader Ibrahim Idriss[1]*

[1]Université de Djibouti, Faculté d'Ingénieurs, GRE, Djibouti, Djibouti

[2]Université de Lyon, CNRS, Université Lyon 1, INSA-Lyon, CETHIL UMR 5008, Villeurbanne, France

Abstract

The current challenge is to reduce the building energy consumption, in hot and humid climates, for which air conditioning is widespread. Up to now, the lack of criteria that identify the available cooling resources and the level of performance of technical solution has represented the major obstacle. To address these issues, the authors propose a new set of indicators to fully inform the decision-making process of the bioclimatic design of fully space-conditioned buildings in a hot and humid climate. This set of indicators provides an overview of the exploitable environmental resource (external air through external convection, natural ventilation and sky radiation cooling) referred as the Environmental Resource Indicators and of the capacity of the building to exploit those resources referred as the Building Performance Indicators. The indicators are implemented for a very basic two-story residential building in the hot, humid climate of Djibouti. The case study shows not only the ability of the indicators to reflect the bioclimatic performances of the buildings but also their ability to give an overview of the building heat exchanges, from which the implication of improper bioclimatic solutions on building cooling consumptions can easily be identified. These indicators are a means to help choose which technical solutions are most suited to the local climate, which is very useful for designers and architects in the early stages of building design.

Keywords: Environmental resources, Climate Indicators, Building Indicators, Bioclimatic Approach, Building Design, Hot Climate

*Corresponding author.

E-mail address: *joseph.virgone@univ-lyon1.fr (Joseph Virgone)

Nomenclature

c_p	specific heat, [kJ/(kg.K)]
φ_{diff}	diffuse radiation, [W/m²]
φ_{dir}	direct radiation, [W/m²]
h_{cv}	convective heat transfer coefficient, [W/(m².K)]
Φ	heat transfer, [W/m²]
Φ_{ac}	sensible cooling flux by air conditioning [W/m²]
Φ_{net}	sum of heat gains to the zone from external wall inner surfaces [W/m²]
Φ_{tr}	transmitted shortwave radiation [W/m²]
I_{night}	night characteristic function
$\dot{V}$	ventilation rate, [m³/s]
V_{bat}	volume of the building [m³]
v_b	basic wind velocity at 10 m above ground level [m/s]
v_{wind}	local wind velocity [m/s]
S	area, [m²]
S_{rhw}	surface representing the entire roof and half of the walls, [m²]
S_{win}	window surface comprising the recommended window-to wall surface [m²]
t	time, [h]
T	temperature, [°C]
T_{ac}	comfort temperature [°C]
$\overset{*}{Q}$	cooling potential (energy quantity), [kWh/m²]
$\overline{Q}_{in}$	internal heat gain (energy quantity), [kWh/m²]
$\hat{Q}$	sheltering potential (energy quantity), [kWh/m²]
$\overline{Q}$	heat input potential (energy quantity), [kWh/m²]
$\overset{*}{Q}^{AC}$	air conditioning needs (energy quantity), [kWh/m²]
Greek symbols	
α	solar absorptance
ρ	density
τ	performance rate
σ	Stefan-Boltzmann constant, [W/(m².K⁴)]
Superscripts	
ref	reference
ENV	environment
EXP	exploited
SHE	sheltered
COV	covered
Subscripts	
a	air
cv	convective exchanges
g	ground
in	indoor
inf	infiltration
out	outdoor
sky	longue wave heat transfer with sky
sun	short wave radiation
vent	ventilation
w	wall
res	resultant
(+)	positive part
(-)	negative part

1. Introduction

In developing countries, the proportion of the urban population is projected to increase from 47% in 2011 to 65% by 2050 (UN-HABITAT). This trend toward urbanization requires the construction of new buildings, but very often, those new buildings are designed without any consideration of energy efficiency and bioclimatic rules. Furthermore, a large number of sub-Saharan African countries do not have energy regulations. Having full air conditioning is considered a basic necessity for these new constructions to be comfortable for occupants all the time in hot countries. These two factors (poor building performance and extensive use of air conditioning) increase the use of energy to achieve thermal comfort. For example, in Djibouti, electricity demand remains dominated by cooling needs and ventilation, which together account for more than 70% of consumption [1].

The principle of passive cooling techniques has been successfully used for centuries, before the appearance of air conditioning. However the economic growth and the standard of living improvement of the population in hot regions have favored the expansion of air conditioning use. Thus, having full air conditioning is considered a basic necessity for new constructions to be comfortable for occupants all the time. The indoor conditions which are achievable in fully bioclimatic buildings are not anymore compatible with the current standard of living that future occupants expect. In this context, a bioclimatic design intends to: a) protect the indoor environment from outdoor heat sources, b) exploit sources of freshness from outdoor environment, and c) make use of thermal inertia to manage the fluctuation of the outdoor freshness availability. We believe that our indicators are suited to quantify the performances of the buildings to follow at least the first two bioclimatic design goals.

For these reasons, bioclimatic design is an alternative solution in new constructions. The ultimate achievement of the bioclimatic design is to obtain a fully passive building, which produce thermal comfort without mechanical system. However, the context of this study is the hot and humid climate [2]. In this context, the weather pattern leads to the widespread use of air-conditioning systems and, thus, high electricity consumption. As a consequence, this paper is restricted to fully space-conditioned buildings in a hot and humid climate. In this context, bioclimatic strategies would take advantage of locally available environmental sources of freshness (air, sky vault or soil) to minimize the cooling energy consumption of the buildings.

Different strategies exist to protect the building from sun heat loads such as shading devices [3–6], surrounding vegetation [7–9], angular and spectral selective coatings [10–18] and double-skin facades or roofs [19–22]. Other technical solutions exist to exploit cooling from the environment, such as night sky cooling systems [23–27], natural ventilation [3,26,28–31] and ground cooling [32–34].

All these techniques need, from early stage of design, devoted analysis tools regarding the amount of available energy they could exploit. These tools are based on their own indicators. The literature proposes many bioclimatic indicators that are focused on the improvement of thermal comfort mostly through natural ventilation [35–47]. It also proposes building performance indicators, but they are mostly component-based [48–51].

None of those indicators is suited to obtain an overview of the whole building performance in the context of the use of bioclimatic resources to reduce cooling energy, except for those developed by Chesné et al. [52], who developed indicators for both the bioclimatic potential of the environment and the building performance for energy reduction in a European climate. Those indicators were based on instantaneous exploitation of environmental resources, and they were generated from building energy simulations by cancelling the effect of some environmental resources. In tropical climates, this technique would lead to unrealistic building thermal behaviors. Additionally, these indicators cannot take into account heat storage in the building envelope. Moreover, their summer indicators are calculated for a free-floating temperature regime within the building.

Thus, new tools are required for both, evaluating the amount of cooling (heating) energy that could be exploited (sheltered) from the environment at a given location, and for assessing the capacity of the building and its systems to exploit (shelter) those environmental cooling resources (heat sources). A simplified overview scheme of the process is given in Fig.1.1.

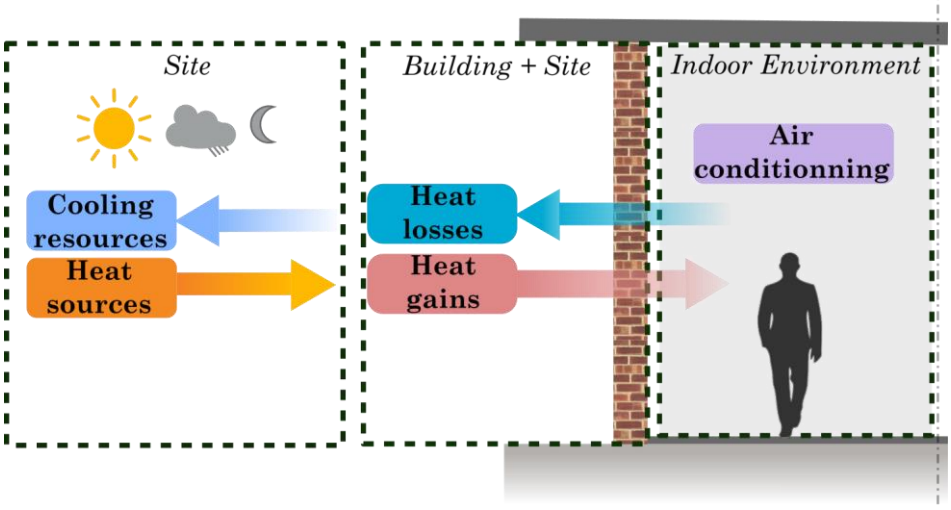

Fig. 1.1. Overview of the idea developed in the article.

The main goal and originality of this article is to define a set of new indicators specifically designed for those purposes. With such a goal in mind, our indicators could be a valuable asset in the bioclimatic design procedure and help the building designers to properly select bioclimatic technologies in the context of using bioclimatic resources to reduce the cooling needs.

The paper is organized as follows: Section two provides a precise definition and identification of a cooling resource for buildings in hot and humid climates. The new sets of bioclimatic indicators are defined in section three. In section four, these indicators are applied to a test case, and the results of the test case are discussed in section five. The paper is concluded in section six by highlighting the key findings and contributions of the study.

2. Identification of the cooling resources

2.1 Definition of a cooling resource

The present paper is focused on buildings with air conditioning systems. A constant value of the temperature set-point of the air conditioning system is assumed throughout the year. This temperature value is named T_{ac}, where ac means "air conditioning".

Thanks to the air conditioning system, the building indoor air temperature is constantly equal to or below T_{ac}. When a building exploits an external cooling resource, it transfers its freshness towards the indoor environment. Thus, an environmental resource can only be exploited as a cooling resource if its characteristic temperature is below T_{ac}. The authors define a cooling resource as an environmental resource whose characteristic temperature is below T_{ac}.

In the rest of the paper, the commonly used value of T_{ac} equal to 26°C is fixed.

Note also that in tropical countries considered in this paper, the level of humidity in the air is too high to enable efficient use of evaporative cooling strategies. Furthermore the use of fans and other low-energy devices are not seen as alternatives but rather as a solution to reduce the cooling needs.

3.2 Identification of the cooling resources

Buildings exchange heat with four environmental elements: the sun, the outdoor air, the outdoor surfaces and the soil. Obviously, the sun will never be a cooling resource; its characteristic temperature is obviously too high.

We assume that the outdoor air temperature $T_{a,out}$ can decrease below T_{ac}. The building exchanges heat with the outdoor air mainly through external convection (on the building envelope) and natural ventilation (through window openings). Since those heat transfer modes are very different, the authors distinguish the outdoor air cooling resource by convection (external convection resource) and by ventilation (ventilation resource).

The buildings exchange heat with the outdoor surfaces by longwave radiation. The external surfaces include the ground, the walls of the surrounding buildings and the sky vault. At the early design stage, it is hardly possible to predict the temperatures of the ground and of the surrounding buildings, but the sky vault temperature T_{sky} might be estimated from meteorological data. The sky vault temperature is nearly always lower than the outdoor air temperature. The sky is considered as a cooling resource.

In hot and humid climates, the deep-ground soil temperature is often very higher than 30°C below 2 m in Djibouti. Temperatures below T_{ac} might be reached only with a limited soil thickness close to the surface and during a limited period of the day. The amount of exploitable cooling energy is very low. The ground will not be investigated any further as a cooling potential. Nevertheless, soil can be cooled below its natural temperature by shading it or by keeping it wet and then be considered as resource.

To summarize, the authors have identified three environmental cooling resources: external convection, ventilation and the sky radiation.

3. Definition of the bioclimatic indicators

3.1 Basic computation principles

Most of the bioclimatic indicators defined in this section are energy potentials. The energy potentials are daily integrations of the incoming/outgoing part of heat fluxes through the building envelope (Fig. 3.1). Let us consider a heat flux Φ passing through the building envelope. The heat flux Φ is positive when the heat flows toward the indoor environment.

The potential $\overset{*}{Q}$ is the integral of the negative part of Φ, which represents a cooling or sheltering potential for the building. The anti-potential $\bar{Q}$ is the integral of the positive part of Φ, and it represents the heat input for the building.

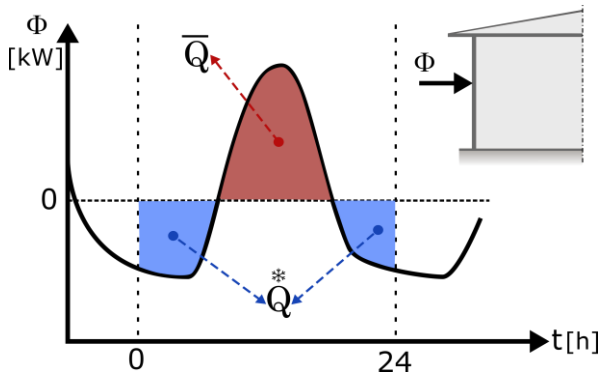

Fig. 3.1. Basic computation principles for the energy potentials

The first set of energy potentials depends only on the construction location and the building dimensions. It evaluates, for each environmental resource, the maximum available cooling energy. The related energy potentials are called “environmental resource indicators”.

The second set of energy potentials evaluates, for each environmental resource, the actual quantity of cooling energy that is utilized by a building, with a specific set of construction solutions. These are principally conceived to orientate the choice of designer toward pertinent solutions that optimize the exploitation of bioclimatic resources. The related energy potentials are called “building performance indicators”.

The third set of indicators provides representative ratios.

3.2 Environment Resource Indicators (ERIs)

The ERIs are computed from a virtual highly permeable building (VHPB) model. The VHPB is a building that has the same dimensions as the building project (e.g., the same number of floors and the same floor areas). It is air-conditioned with T_{ac} as the temperature set-point. Its envelope is designed to maximize the heat exchanges with the external environment.

The thermal resistance of the VHPB envelope is null. The only thermal resistance between the indoor and the outdoor environment is due to the external convection heat transfer. Thus, the temperature of the VHPB envelope is constant and equal to T_{ac}. The albedo of the VHPB envelope is equal to 0. Its longwave emissivity is equal to 1. The VHPB is supposed to be a single building on a flat surface: there is no external shading element.

The VHPB orientation is such that its widest side is always perpendicular to the wind direction to maximize the natural ventilation flow rate. The literature suggests that the window-to-wall ratio (WWR) of buildings should not exceed 15% in hot climates [3,53,54] to avoid excessive solar loads within the building. The VHPB follows this suggestion: the

surface of the windows S_{wind} is equal to 15% of the total wall surfaces. The windows are distributed equally over the windward ($S_{wind}/2$) and the leeward ($S_{wind}/2$) walls of the VHPB. The windows are opened only when the outdoor air temperature is below T_{ac}. The VHPB is used to compute the environmental cooling potentials $\overset{*}{Q}^{ENV}$ and the environmental heat input potentials $\bar{Q}^{ENV}$. A complete overview of the ERIs is given in Fig. 3.2. $\overset{*}{Q}^{ENV}_{sky}$, $\overset{*}{Q}^{ENV}_{cv}$, $\overset{*}{Q}^{ENV}_{vent}$ and $\overset{*}{Q}^{ENV}_{g}$ are the environmental cooling potentials from the sky vault, the external convection, the natural ventilation and the ground, respectively. $\bar{Q}^{ENV}_{sun}$, $\bar{Q}^{ENV}_{cv}$, and $\bar{Q}^{ENV}_{sky}$ are the environmental heat input potentials from the sun, the outdoor air (external convection) and the sky vault, respectively. The present paper focus only on the cooling potentials $\overset{*}{Q}^{ENV}_{sky}$, $\overset{*}{Q}^{ENV}_{cv}$ and $\overset{*}{Q}^{ENV}_{vent}$ and on the sun heat input potentials $\bar{Q}^{ENV}_{sun}$.

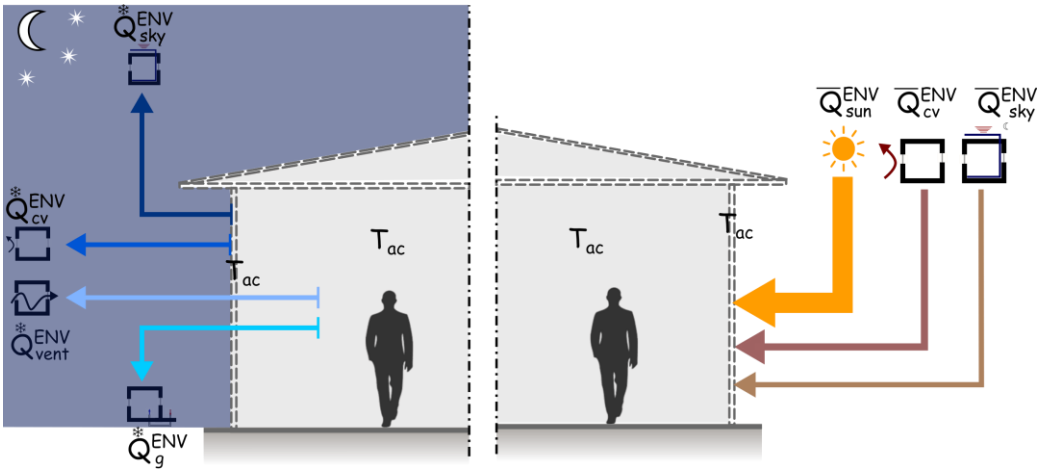

Fig. 3.2. The environmental resource indicators

The environmental sun heat input potential is the daily integration of the direct and diffuse solar radiation absorbed by each wall of the VHPB:

$$\bar{Q}^{ENV}_{cv} = \int_0^{24} \Phi_{sun} dt \tag{1}$$

$$\text{with } \Phi_{sun} = \sum_w \left(\varphi_{diff} + \varphi_{dir_w}\right) S_w \tag{2}$$

where φ_{diff} represents the diffuse radiation, φ_{dir_w} the direct radiation on each wall and roof, and S_w the surface of each wall and roof.

The external convection Φ^{ref}_{cv} and the longwave sky radiation Φ^{ref}_{sky} heat flux over the VHPB are given by the following expressions:

$$\Phi^{ref}_{cv} = S_w \cdot h_{cv} \cdot \left(T_{a_{out}} - T_{ac}\right) \tag{3}$$

$$\Phi^{ref}_{sky} = S_{rhw} \cdot \sigma \cdot \left(T^4_{sky} - T^4_{ac}\right) \tag{4}$$

To estimate the convective heat transfer coefficient h_{cv}, the following correlation provided by Mac Adams [55] is used:

$$h_{cv} = 5.7 + 3.8 v_{wind} \quad (5)$$

In Eq. 4, the surface S_{rhw} is the surface of the roof plus half of the walls' surfaces. Indeed, the walls exchange longwave radiation with the surrounding surfaces and the sky. By setting $S_{rhw} = S_w/2$, half of these longwave radiation exchanges are due to interactions with the sky.

The external convection and sky environmental cooling potentials are computed by integrating, over the night only, the negative parts of Φ_{cv}^{ref} and Φ_{sky}^{ref}:

$$\overset{*}{Q}_{cv}^{ENV} = \int_0^{24} \left|\Phi_{cv-}^{ref}\right| \cdot I_{night} \cdot dt \quad (8)$$

$$\overset{*}{Q}_{sky}^{ENV} = \int_0^{24} \left|\Phi_{sky-}^{ref}\right| \cdot I_{night} \cdot dt \quad (9)$$

Here, I_{night} is a function that is equal to 0 when sun radiation is present and 1 when there is no radiation from the sun. With this restriction, it is assumed that the convection and sky cooling potentials could only be exploited when the building envelope is not heated by sun radiation. The authors assume that, during the day, the longwave radiation and the convection heat flux mostly compensate the solar radiation rather than cool down the inside environment of the building.

The natural ventilation environmental cooling potential is defined as the negative value of the daily enthalpy flow exchanged between the outside and the inside air of the VHPB.

$$\overset{*}{Q}_{vent}^{ENV} = \int_0^{24} \left|\Phi_{vent-}^{ref}\right| \cdot dt \quad (10)$$

where,

$$\Phi_{vent}^{ref} = cp_a \cdot \rho_a \cdot \dot{V}^{ref} \cdot \left(T_{a_{out}} - T_{ac}\right) \quad (11)$$

The ventilation flow rate in the VHPB, $\dot{V}^{ref}$, is calculated with Eq. 12:

$$\dot{V}^{ref} = \min\left[\frac{C_d \cdot S_{wind}}{2\sqrt{2}} \cdot \sqrt{\Delta C_p} \cdot v_{wind}\,; \frac{10 \cdot V_{bat}}{3600}\right] \quad (12)$$

Here, C_d is the discharge coefficient of the window openings, ΔC_p is the difference of wind pressure coefficient between the windward and the leeward walls, and v_{wind} is the mean wind velocity at roof height. The discharge coefficient is taken as $C_d = 0.6$. Given the orientation of the VHPB, the wind pressure coefficients may be estimated as 0.5 on the windward wall and -0.7 on the leeward wall. Thus, ΔC_p is equal to 1.2.

We fixed a maximum value of 10 ach (air change per hour) for the ventilation flow rate. This maximum value is defined as the attainable air flow rate using commonly existing natural ventilation strategies in the literature review [52,56,57]. It is also the limit from which too large air velocity is encountered inside the building.

The local wind velocity v_{wind} is estimated from the logarithmic law of Von Karman adapted in Eurocode 1:

$$v_{wind} = v_b \cdot c_r(z) \tag{13}$$

where v_b corresponds to the measured wind velocity at 10 m above ground level. $c_r(z)$ is the terrain roughness coefficient, which considers the height above ground and the ground roughness of terrain upwind:

$$c_r(z) = \begin{cases} k_r \, ln\left(\frac{z}{z_0}\right) & z_{min} \leq z \leq z_{max} \\ c_r(z_{min}) & z \leq z_{min} \end{cases} \tag{14}$$

$$k_r = 0.19 \left(\frac{z_0}{0.05}\right)^{0.07} \tag{15}$$

Here, z_0 is the roughness length, k_r is a terrain factor that depends on z_0, z_{min} is the minimum height depending on the terrain category, and z_{max} is equal to 200 m.

Building Performance Indicators (BPIs)

The BPIs are calculated from building energy simulation outputs (BES). BES programs (EnergyPlus, Trnsys, DO2, etc.) provide access to all the computed heat fluxes that are needed to compute the BPI.

A complete overview of the BPIs is illustrated in Fig. 3.3. The BPIs are named Q^{EXP}, where "EXP" means "exploited potentials". Since the heat flux amplitudes are much larger on the exterior surface than on the interior surface of the building envelope, the study distinguish between the outdoor and indoor exploited potentials.

For the outdoor side, $\bar{Q}_{sun}^{ENV}$, $\bar{Q}_{cv}^{EXP}$ and $\bar{Q}_{sky}^{EXP}$ represent the heat input potentials by shortwave radiation, convection and longwave radiation, respectively (including the heat exchanges with the sky and the other surfaces of the environment). $\hat{Q}_{sun}^{EXP}$, $\hat{Q}_{cv}^{EXP}$ and $\hat{Q}_{sky}^{EXP}$ are the sheltering potentials. They are named the sheltering potentials because they mostly compensate the heat inputs; they rarely refresh the indoor environment. The sheltering effect is symbolized by the hat symbol over the letter $\hat{Q}$.

For the indoor exploited potentials, it is quite difficult to distinguish between the shortwave radiation, the longwave radiation and the external convection components of the heat flux transmitted by the envelope. The residual exploited potential $\overset{*}{Q}_{res}^{EXP}$ results

from convective and radiative cooling on the external side of the envelope. The exploited heat input potential $\bar{Q}_{res}^{EXP}$ results from convection, longwave radiation and sun radiation heating on the external face of the building, including the shortwave radiation that passes through the windows. The potential $\overset{*}{Q}_{vent}^{EXP}$ is the exploited natural ventilation potential, and $\overset{*}{Q}^{AC}$ is the cooling power provided by the air conditioning system to maintain the internal temperature below T_{ac}.

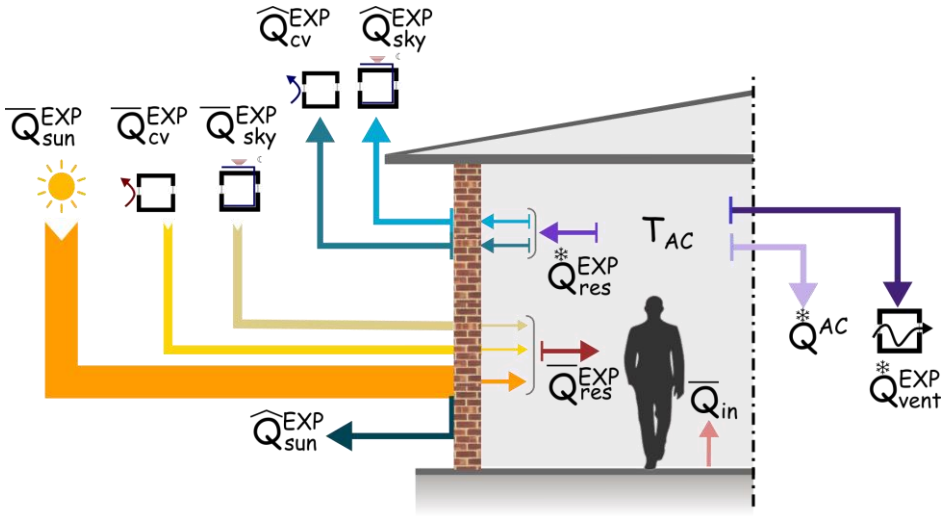

Fig. 3.3. The building performance indicators for the design stage

Building energy simulations provide output values for the convection heat flux Φ_{cv} and the net longwave heat flux Φ_{lw} over the external surface of the building envelope. The fluxes are negative when the heat goes outdoors. The outdoor potentials are computed as follows:

$$\hat{Q}_{sun}^{EXP} = (1-\alpha)\bar{Q}_{sun}^{ENV} \tag{16}$$

$$\hat{Q}_{sky}^{EXP} = \int_0^{24} |\Phi_{lw-}|\, dt \tag{17}$$

$$\hat{Q}_{cv}^{EXP} = \int_0^{24} |\Phi_{cv-}|\, dt \tag{18}$$

$$\bar{Q}_{sky}^{EXP} = \int_0^{24} \Phi_{lw+}\, dt \tag{19}$$

$$\bar{Q}_{cv}^{EXP} = \int_0^{24} \Phi_{cv+}\, dt \tag{20}$$

The subscripts + and – respectively indicate that only the positive or the negative part of the fluxes is retained.

BES also provides outputs for the residual (conduction) heat flux through the inner surface of the envelope $\Phi_{net_{in}}$, the heat flux by infiltration Φ_{inf}, the natural ventilation Φ_{vent} and

the air conditioning cooling production Φ_{ac}. The indoor exploited cooling potentials are computed as follows:

$$\overset{*}{Q}_{res}^{EXP} = \int_0^{24} \left|\Phi_{net_{in-}}\right| dt \quad (21)$$

$$\overset{*}{Q}_{vent}^{EXP} = \int_0^{24} \left|\Phi_{inf-} + \Phi_{vent-}\right| dt \quad (22)$$

$$\overset{*}{Q}^{AC} = \int_0^{24} \left|\Phi_{ac}\right| dt \quad (23)$$

$\bar{Q}_{res}^{EXP}$ is the actual amount of heat that travels through the envelope and reaches the indoor environment. It is computed from the positive values of $\Phi_{net_{in}}$ and the internal shortwave radiation heat loads Φ_{tr} from BES:

$$\bar{Q}_{res}^{EXP} = \int_0^{24} \left(\Phi_{net_{in+}} + \Phi_{tr}\right) dt \quad (24)$$

The indoor energy balance sets that the heat inputs from the envelope $\bar{Q}_{res}^{EXP}$ and from the internal loads $\bar{Q}_{in}$ are compensated by the cooling energy from outdoor through the envelope Q_{res}^{EXP}, through the natural ventilation $\overset{*}{Q}_{vent}^{EXP}$ and by the cooling energy provided by the air conditioning system $\overset{*}{Q}^{AC}$. This results in the indoor balance equation:

$$\bar{Q}_{res}^{EXP} + \bar{Q}_{in}^{EXP} = \overset{*}{Q}_{res}^{EXP} + \overset{*}{Q}_{vent}^{EXP} + \overset{*}{Q}^{AC} \quad (25)$$

Performance ratios

The capacity of a building to transfer outdoor cooling resources to the indoor environment is quantified by three ratios: the cover rate, the exploitation rate and the sheltering rate.

The cover rate relates the exploited cooling energy from a specific resource to the internal heat loads through the envelope $\overline{Q}_{res}^{EXP}$. It is named τ^{COV} with the name of the resource in subscript (*vent* for natural ventilation, or *res* for the residual flux through the envelope). It is calculated as follows:

$$\tau^{COV} = \frac{\overset{*}{Q}^{EXP}}{\bar{Q}_{res}^{EXP}} \quad (26)$$

The exploitation rate relates the exploited cooling energy from a specific resource to the environmental cooling energy that would be exploitable for that specific resource. It is named τ^{EXP} with the name of the resource in subscript (*vent* for natural ventilation, or *res* for residual flux through the envelope). It is calculated as follows:

$$\tau^{EXP} = \frac{\overset{*}{Q}^{EXP}}{Q^{ENV}} \tag{27}$$

The sheltering rate represents the capacity of the envelope to act as a barrier facing the external heat sources. The sheltering rate is defined as follows:

$$\tau^{SHE} = \frac{\hat{Q}_{sun}^{RFX} + \hat{Q}_{sky}^{EXP} + \hat{Q}_{cv}^{EXP}}{\left(\bar{Q}_{sun}^{ENV} + \bar{Q}_{sky}^{EXP} + \bar{Q}_{cv}^{EXP}\right)} \tag{28}$$

A simplified scheme of the indicators developed in this paper is given in Fig. 3.4.

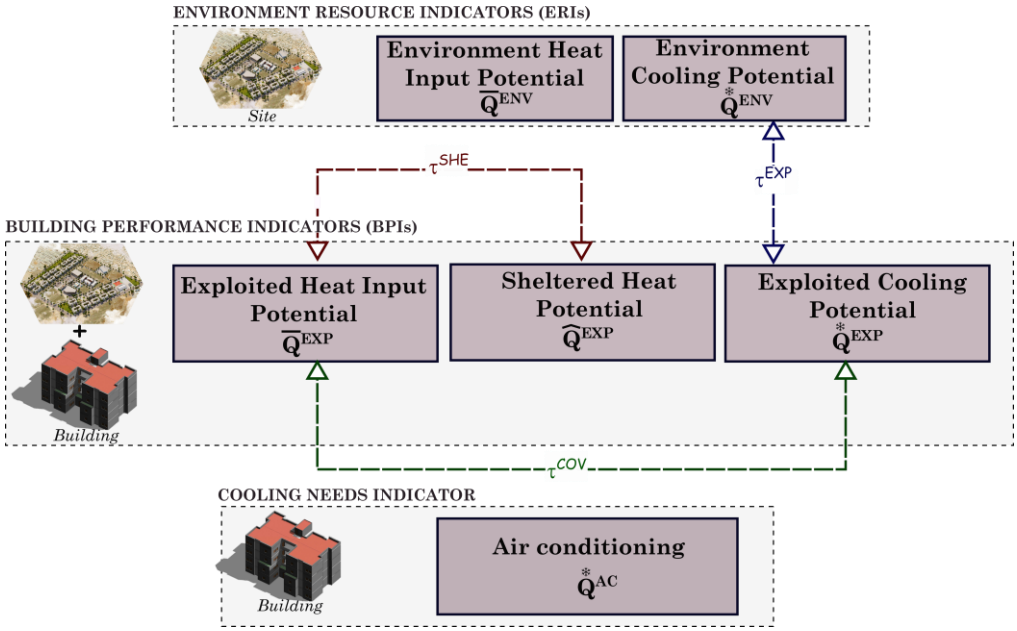

Fig. 3.4. Overview of the indicators

4. Case Study

In this section, the authors illustrate the use of bioclimatic indicators through a case study. The case study is a generic two-story building located in Djibouti. The main purpose of this case study is to show the nature of the information that can be drawn from the analysis of the indicator values and to demonstrate their applicability to different wall configurations.

4.1 Description of the test case

4.1.1 Weather data for Djibouti

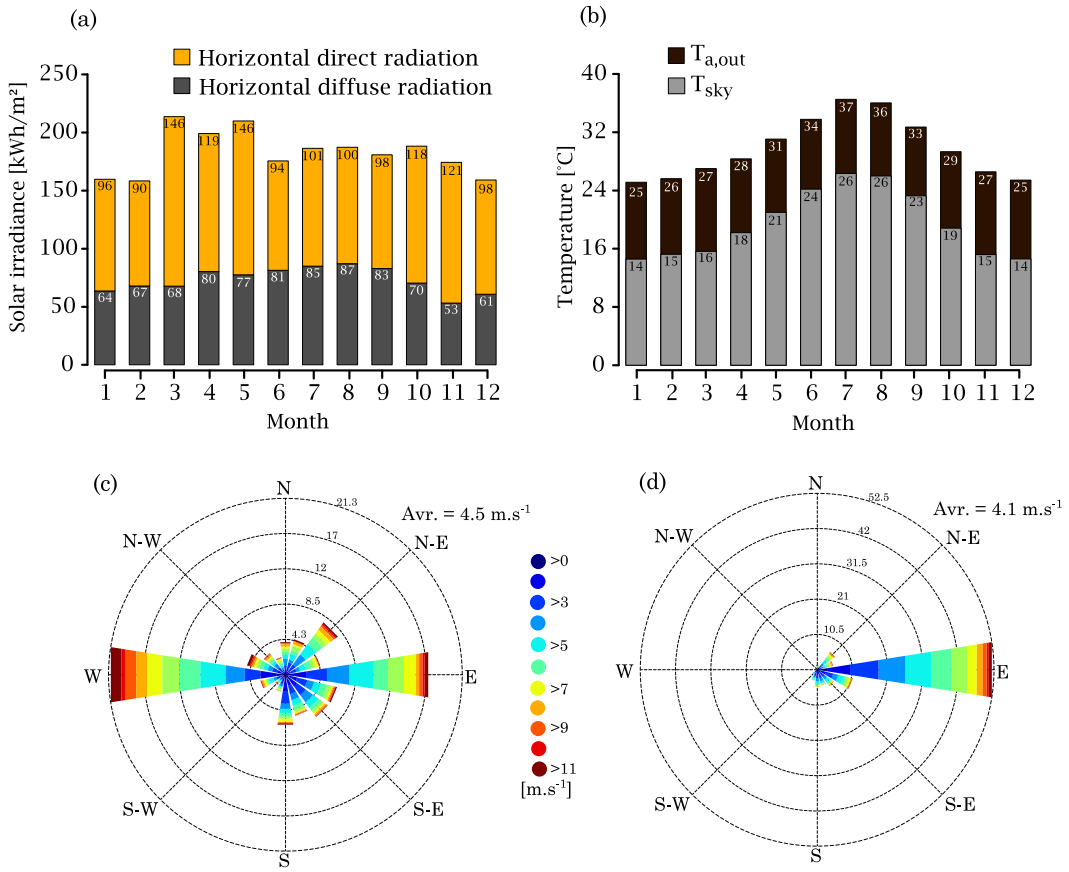

Fig. 4.1. Weather data in Djibouti (a) Monthly solar radiation, (b) Monthly mean temperatures of the air and the sky, (c) Wind rose for the cool season and (d) Wind rose for the hot season

Characteristic features of the weather of Djibouti are displayed in Fig. 4.1. The monthly distribution of solar radiation is displayed in Fig. 4.1a. The solar radiation is constantly high throughout the year (more than 150 kWh/m².month and up to 200 kWh/m².month all year). The direct radiation represents the major part of the solar radiation (on average, 60%).

The monthly distributions of the outdoor air and sky temperatures are displayed in Fig. 4.1b. The sky temperature was determined using an equation suggested by Centeno [58] and Clark and Allen [59]. The sky temperature is often lower than the ambient air temperature, and the difference is higher between November and March.

The weather of Djibouti is characterized by very low rainfall and very high humidity [2,60]. The monthly averaged outdoor air temperatures oscillate between 25°C and 35°C. The cool season, from November to March, is hot and very humid, with an east trade wind coming

from the sea (Fig. 4.1c). During this season, the humidity content does not fall below 70%. The summer season, from April to October, is very hot and slightly dryer, with west prevailing winds coming from the continent at a low speed (< 5 m/s), as shown in Fig. 4.1d.

4.1.2 Building configurations

Fig. 4.2 shows a 3D visualization of the test case building. It is a generic two-story building model. It was modeled using DesignBuilder software (EnergyPlus), which is a validated program for building energy simulation. Its floor dimensions are 8 m × 10 m. The building height is 7 m. The total cooled floor area is 160 m², and the total cooling volume is 560 m³.

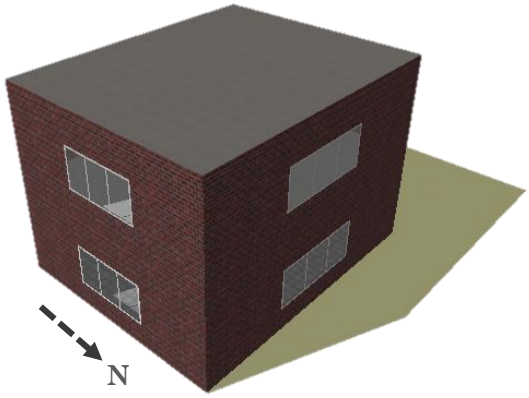

Fig. 4.2. Geometry of the test case building

The building has been simulated with four extreme versions of envelope compositions, delimiting the scope of the study. The thermal inertia of the envelope has been varied from lightweight to heavyweight and the insulation from "no insulation" to "insulated". The envelope compositions below are given from the outer layer to the inner layer.

Heavyweight and Insulated (HWI):

- Walls: 10 cm brickwork, 12 cm extruded polystyrene, 10 cm concrete blocks and internal rendering (U = 0.25 W/m². K)
- Roof: 2 cm asphalt, 1.3 cm fiberboard, 20 cm extruded polystyrene and 10 cm cast concrete (U = 0.15 W/m². K)
- Floor slab: 25 cm urea formaldehyde foam, 10 cm cast concrete, 5 cm floor screed and floor tiles (U = 0.15 W/m². K)

Heavyweight, no Insulation (HWnoI):

- Walls: 10 cm brickwork, 10 cm concrete blocks and internal rendering (U = 2.56 W/ m². K)
- Roof: 2 cm asphalt, 1.3 cm fiberboard and 10 cm cast concrete (U = 3.8 W/m². K)

- Floor slab: 10 cm cast concrete, 5 cm floor screed and floor tiles (U = 2.5 W/m². K)

Lightweight and Insulated (LWI):

- Walls: 0.6 cm lightweight metallic cladding, 13 cm extruded polystyrene, and 1.3 cm gypsum plastering (U = 0.25 W/m². K)
- Roof: 1 cm metal deck, 22 cm extruded polystyrene and metal surface (U = 0.15 W/m². K)
- Floor slab: 25 cm urea formaldehyde foam, 10 cm cast concrete, 5 cm floor screed and floor tiles (U = 0.15 W/m². K)

Lightweight, no Insulation (LWnoI):

- Walls: 0.6 cm lightweight metallic cladding (U = 5.8 W/ m². K)
- Roof: 1 cm metal deck and metal surface (U = 7.2 W/m². K)
- Floor slab: 10 cm cast concrete, 5 cm floor screed and floor tiles (U = 2.3 W/m². K)

The glazing properties as well as the window to wall ratio of the archetypical buildings are presented in Table 2.

Table 1. Glazing properties.

	Description	U-Value [W/m². K]	SHGC*	WWR [%]
LWI & HWI	low-emissivity double (with air filled cavity)	1.8	0.6	15
LWnoI & HWnoI	single	5.8	0.83	15

* Solar Heat Gain Coefficient.

The solar absorptance values of the walls and roof are set to 0.7 and 0.85, respectively. The infiltration flow rates are set to 0.5 ach. Natural ventilation is active, and the operable windows open only when the conditions are favorable, i.e., when the outdoor temperature is lower than T_{ac} and the air-conditioning system is off.

An occupancy scenario is integrated into the simulation. Table 1 gives the total internal loads (occupants and electric devices) for one day.

Table 2. Daily occupancy and internal heat.

0 h - 5 h	6 h - 7 h	8 h - 17 h	18 h - 19	20 h - 22 h	23 h -0 h
3 W/m²	7 W/m²	5 W/m²	h 18 W/m²	20 W/m²	18 W/m²

4.2 Results

Here, the energy potentials are presented as annual potentials (sum over the year of the daily potentials) or monthly averaged potentials (average over the month of the daily potentials). All the energy potentials were divided by the total cooled floor area.

4.2.1 Environmental resources

Fig. 4.3 displays the monthly average of the environmental cooling potentials available in the site for the sky ($\overset{*}{Q}_{sky}^{TOT}$) the external convection ($\overset{*}{Q}_{cv}^{TOT}$) and natural ventilation ($\overset{*}{Q}_{vent}^{TOT}$) resources. Generally, all resources are available during the cool season. Nevertheless, the sky stands out from other resources. It is by far the resource that provides the most cooling energy with a maximum of 1,400 Wh/m² on average per day in January. This resource also lasts longer than the others and reaches a minimum of 200 Wh/m² for July and August. During the hot season, the air resources (external convection and natural ventilation) become heat sources. The external convection and the natural ventilation potentials have similar amplitudes during the cool season.

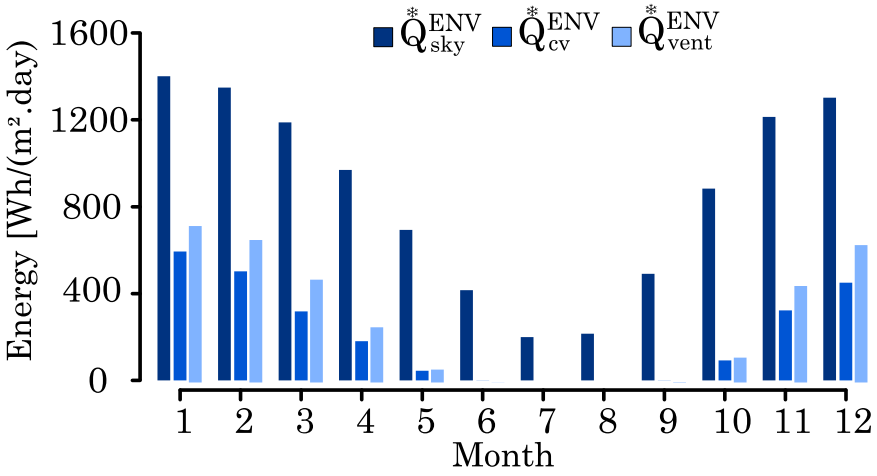

Fig. 4.3. Monthly distribution of the environmental cooling potentials for all the resources.

The sun heat input potential of the site, $\overline{Q}_{sun}^{TOT}$, is illustrated in Fig. 4.4. It is constantly high throughout the year (between 7 kWh/m².day and 8 kWh/m².day). Furthermore, the sum of the environmental cooling potentials is significantly lower than $\overline{Q}_{sun}^{TOT}$, even more in the summer than in the cool season. The site is characterized by more heat input than cooling benefit available all the year.

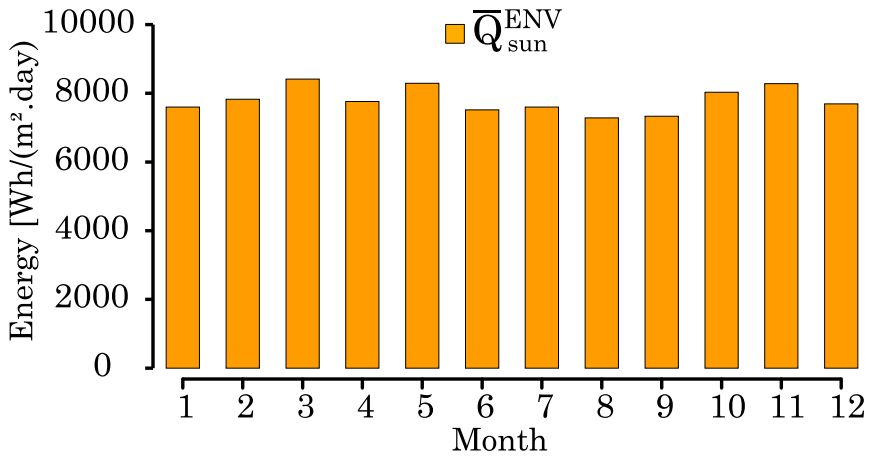

Fig. 4.4. Monthly distribution of the environmental heat input potential of the sun.

4.2.2 Evaluation of the building designs

4.2.2.1 Annual observations

Fig. 4.5 shows the environmental cooling potentials $\overset{*}{Q}^{ENV}$, the exploited cooling potentials $\overset{*}{Q}^{EXP}$, the exploitation rates τ^{EXP}, the cover rates τ^{COV} for the sky + convection cooling resources and the ventilation cooling resource for the four building configurations. The sky and the external convection environmental cooling potentials ($\overset{*}{Q}^{ENV}_{sky}$ and $\overset{*}{Q}^{ENV}_{cv}$) were added to be compared to the indoor residual cooling potential $\overset{*}{Q}^{EXP}_{res}$.

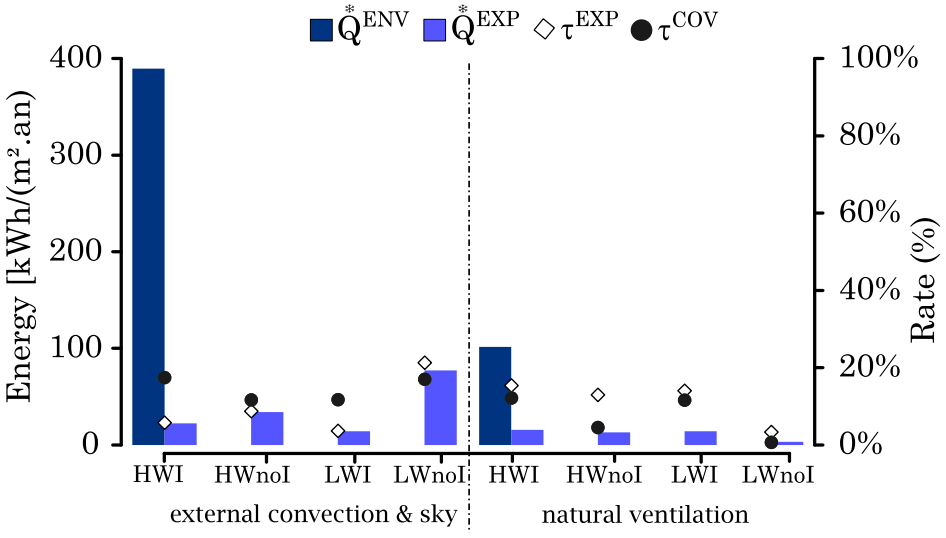

Fig. 4.5. Environmental and exploited annual cooling potentials for the external convection and sky resources and for the natural ventilation resource. Comparison of the different envelope configurations.

In all cases, the available cooling energy in the site $\overset{*}{Q}^{ENV}$ far exceeds the exploited cooling energy $\overset{*}{Q}^{EXP}$, which partly explains the low values of the exploited rate and the cover rate. The different envelope compositions display different behaviors.

For the external convection and sky resources, the exploited cooling potential $\overset{*}{Q}_{res}^{EXP}$ and the exploitation rate τ_{res}^{EXP} are higher for non-insulated buildings, with a maximum of 22% for the LWnoI configuration. This is because the non-insulated building transfers the outdoor cooling energy more easily through the envelope. However, non-insulated envelopes also transfer more heat toward the indoor environment. The heat input energy $\bar{Q}_{res}^{EXP}$ is higher, which is why the coverage ratio τ_{res}^{COV} is not systematically higher for non-insulated buildings. For buildings with high insulation, the exploitation rate τ_{res}^{EXP} never exceeds 5%; insulated building envelopes cannot transfer more than 5% of the cooling energy available on their external surfaces.

The thermal inertia damps the oscillations of the residual heat flux at the inner surface of the envelope $\Phi_{net_{in}}$. The heat flux reaches less extreme negative values. That is why the residual exploited potentials $\overset{*}{Q}_{res}^{EXP}$ are much lower for buildings with higher inertia.

For the natural ventilation resource, the highest exploitation rates τ_{vent}^{EXP} are found for the buildings with high thermal inertia and high insulation. The exploited ventilation potential $\overset{*}{Q}_{vent}^{EXP}$ is proportional to the indoor-outdoor temperature difference $T_{a_{in}} - T_{a_{out}}$, with $T_{a_{in}} > T_{a_{out}}$. Thus, the exploited ventilation potential Q_{vent}^{EXP} is lower if the indoor temperature $T_{a_{in}}$ decreases too quickly when the fresh air enters the room. Building with high inertia slows down the decrease of $T_{a_{in}}$ by absorbing a portion of freshness within the building structure. Buildings with no insulation seem to accelerate the decrease of $T_{a_{in}}$. This decrease might be due to additional heat losses through the envelope, which results from the exploitation of the sky and external convection resources. This explanation supposes that there is a synchronization between the availability of the ventilation resource and the external convection and sky resources.

Fig. 4.6 shows the annual external heat input and sheltering potentials for the 4 building configurations. The environment external heat input potential $\bar{Q}^{ENV}$ is the sum of the short wave radiation, convection, and longwave radiation potentials ($\bar{Q}_{sun}^{ENV}$, $\bar{Q}_{cv}^{EXP}$ and $\bar{Q}_{sky}^{EXP}$). The environment sheltering potential $\hat{Q}^{EXP}$ is the sum of the sheltering potentials $\hat{Q}_{sun}^{EXP}$, $\hat{Q}_{cv}^{EXP}$ and $\hat{Q}_{sky}^{EXP}$. Fig. 4.6 also shows the sheltering rate of the buildings.

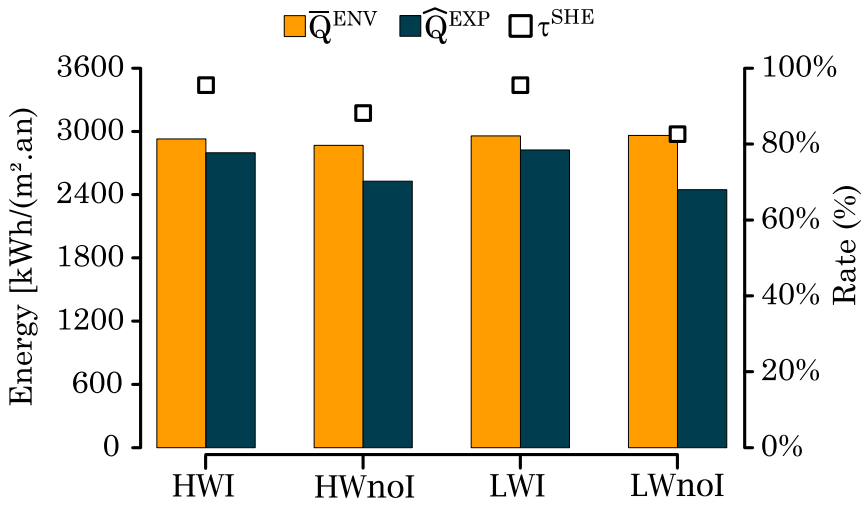

Fig. 4.6. Annual external exploited heat input and shelter potentials. Comparison between four envelope configurations.

The sheltering rate τ^{SHE} is over 80% for all cases. Thus, at least 80% of the external heat input $\bar{Q}^{EXP}$ is sheltered by the building envelope and does not reach the indoor environment. As noted earlier, the difference between $\bar{Q}^{EXP}$ and $\hat{Q}^{EXP}$ represents the indoor residual heat input $\bar{Q}_{res}^{EXP}$, i.e., the portion of the heat that the building will have to evacuate by exploiting cooling resources (convection, sky and ventilation) and by using the air conditioning system.

The environment external heat input potential $\bar{Q}^{ENV}$ is homogeneous between the four envelope configurations. The different behaviors are found in the values of the sheltering potential $\hat{Q}^{EXP}$. This potential is much higher for buildings with thermal insulation and becomes slightly higher when thermal inertia is added. When a building is heavily insulated, its external surface temperature $T_{w_{out}}$ is very high, which results in high values of convection and longwave radiation heat flux toward the outdoor environment. Please note that for the HWI configuration, the sheltering rate τ^{SHE} reaches 96%. Only 4% of the heat input reaches the indoor environment.

Fig. 4.7 shows the decomposition of the outdoor (left-side) and indoor (right-side) potentials for the four building configurations. Each subfigure provides a snapshot of the year-round bioclimatic performances of a particular building configuration. The vertical scale is different between the indoor and outdoor indicators because the orders of magnitude of the fluxes are different.

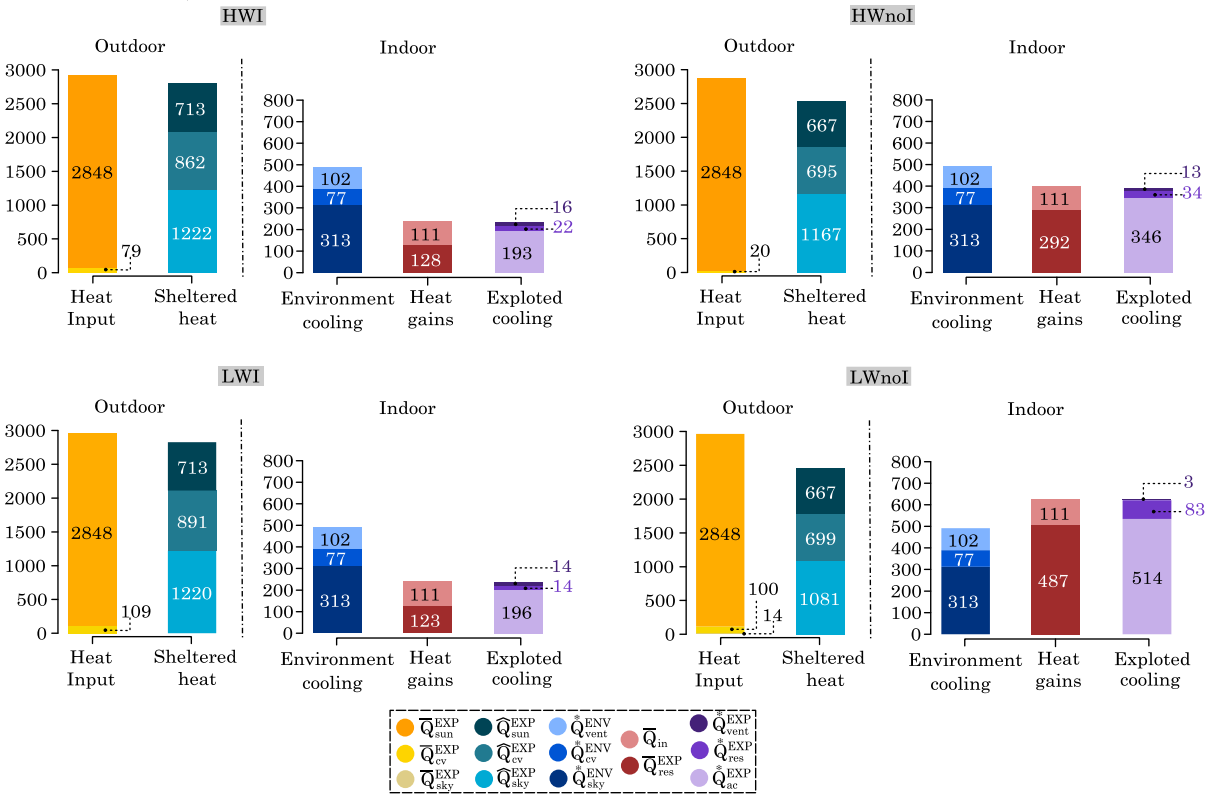

Fig. 4.7. Comparison between the annual ERIs and BPIs (kWh.m².an^{-1}) for the four envelope compositions.

$\bar{Q}_{cv}^{EXP}$ is systematically very low compared to $\bar{Q}_{sun}^{EXP}$, and $\bar{Q}_{sky}^{EXP}$ is almost always equal to zero. Most of the building heat input comes directly from sun radiation. The external surface temperature rarely decreases below the external air temperature, especially when the envelope has high thermal inertia.

For all the buildings, the sky sheltering potential $\hat{Q}_{sky}^{EXP}$ is the largest among the three sheltering potentials $\hat{Q}_{sun}^{EXP}$, $\hat{Q}_{sky}^{EXP}$ and $\hat{Q}_{cv}^{EXP}$. A large part of the incoming radiation is directly reflected by the envelope. Then, it is evacuated to the outdoor environment by longwave radiation and convection. The fact that the convection sheltering potential $\hat{Q}_{cv}^{EXP}$ is lower than the sky sheltering potential $\hat{Q}_{sky}^{EXP}$ is valuable because the energy associated with $\hat{Q}_{cv}^{EXP}$ directly heats up the air around the building, which might result in outdoor discomfort near the building.

For each building configuration, the sum of the environmental cooling potentials $\overset{*}{Q}_{vent}^{ENV} + \overset{*}{Q}_{cv}^{ENV} + \overset{*}{Q}_{sky}^{ENV}$ is systematically higher than the sum of the heat inputs through the envelope and the internal loads $\bar{Q}_{res}^{EXP} + \bar{Q}_{in}$, except for LWnoI. In principle, bioclimatic resources should globally be able to cover cooling demands if they could be properly exploited.

We retrieve the indoor heat balance (Eq. 24) from the values of the indoor exploited potentials. Buildings with low insulation exploit more of the external convection + sky resources ($\overset{*}{Q}_{res}^{EXP}$ is higher), but they expose more of the indoor environment to external heat loads ($\bar{Q}_{res}^{EXP}$ higher), which results in higher air conditioning consumption ($\overset{*}{Q}^{AC}$ is higher).

4.2.2.2 Dynamic analysis

Fig. 12 shows the monthly average of indicators for the external convection and sky resources for each version of buildings. Fig. 4.8 shows the monthly average indicators of the ventilation resource for each version of buildings. Fig 4.9 shows the monthly average residual incoming heat energy through the envelope, $\bar{Q}_{res}^{EXP}$, for all versions of buildings. In each figure, the hot season is identified by a red background.

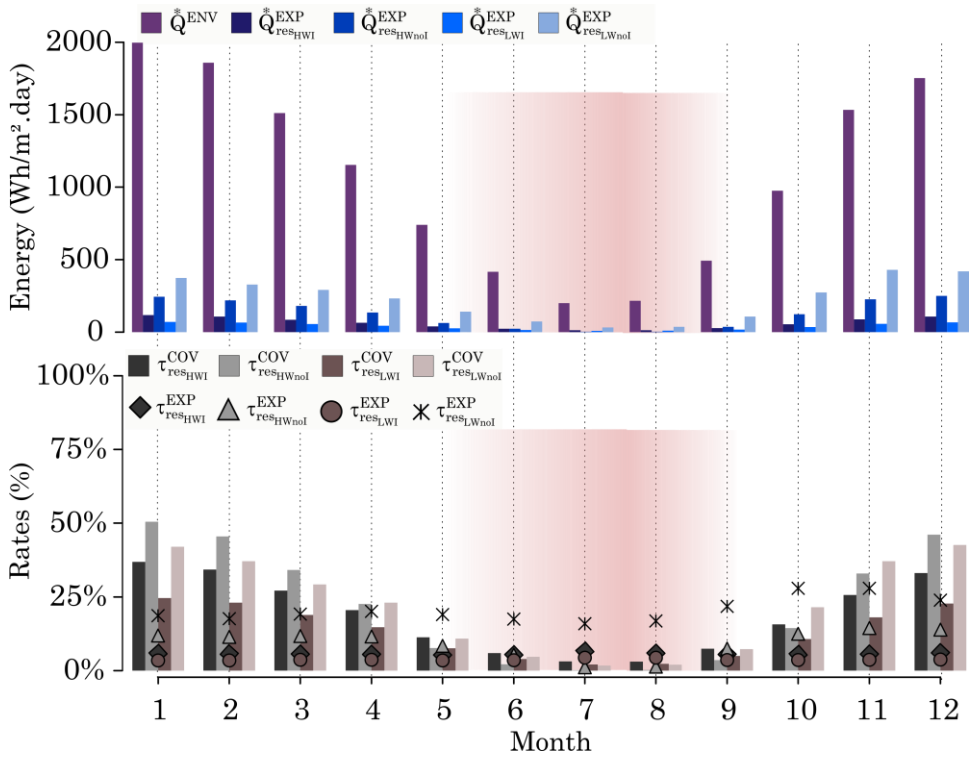

Fig. 4.8. Monthly averages of the external convection + sky indicators for all buildings.

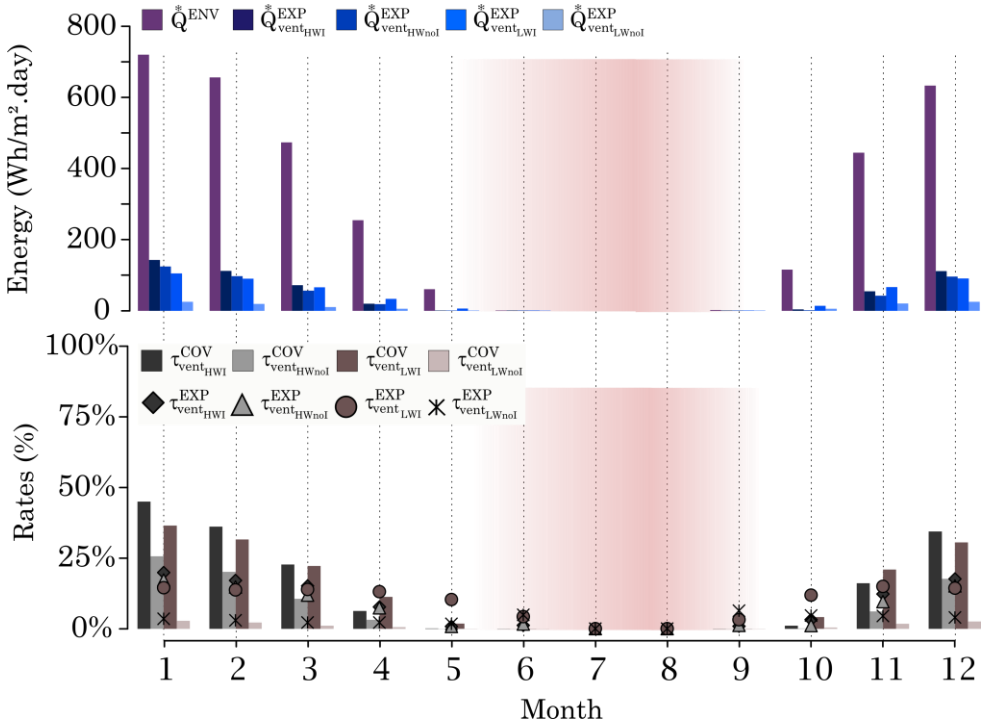

Fig. 4.9. Monthly averages of the ventilation indicators for all buildings.

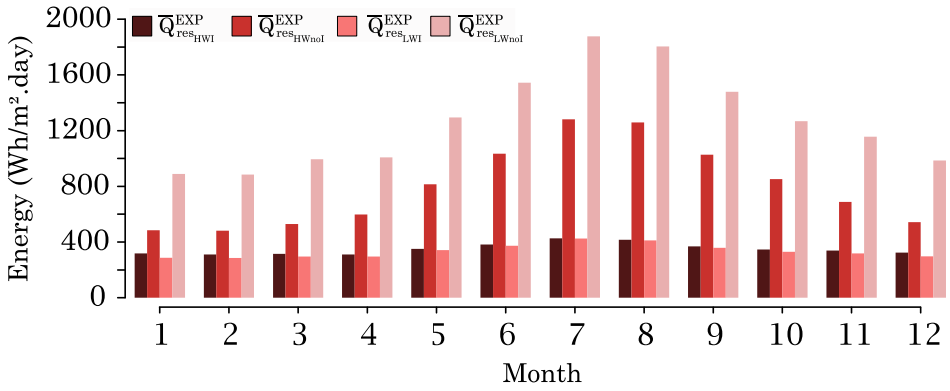

Fig. 4.10. Monthly averages of the residual heat input potentials for the four building configurations.

During the hot season, the environmental cooling potentials are almost zero. Only the LWnoI building configuration exploits a fraction of the available freshness from the external convection + sky resource: $\tau^{EXP}_{res_{LWnoI}}$ = 17% in August (Fig. 4.8). However, this is at the expense of a very high residual heat input (Fig. 4.10).

During the cool season, the sum of the coverage potentials $\tau^{COV}_{res} + \tau^{COV}_{vent}$ reaches 80% for the HWI configuration and 50% for the LWnoI configuration. More than half of the building heat loads are compensated by the cooling resources. The repartition of the covering ratio is different for both configurations: the HWI building mainly exploits the ventilation resource when the LWnoI mainly exploits the external convection and sky resources.

Generally, only the LWnoI configuration significantly exploits the convection and sky resources over the year (Fig. 4.8). The exploited ratio τ_{res}^{EXP} oscillates between 15% and 30% throughout the year for the LWnoI configuration; it never exceeds 15% for the HWnoI configuration and 5% for the other configurations. The LWnoI building exploits less of the ventilation resources than the other building configurations between October and May.

Fig. 14 confirms that, on average, $\bar{Q}_{res}^{EXP}$ is higher for the non-insulated building configurations. It also reveals that the amplitudes of the variations of $\bar{Q}_{res}^{EXP}$ are also greater for those configurations.

5. Discussions

In the previous section, the authors performed a physical interpretation of the indicator values that demonstrated the indicators consistency with physical considerations. In the present section, the nature of the decisions that could be drawn from an analysis of the indicator values within the framework of a building project is shown.

The observation of the environmental resource indicators revealed the quasi-absence of cooling resources during the hot season. This information is clearly valuable for building engineers because it excludes the possibility to base the cooling strategy of the building only on the exploitation of the bioclimatic resources unless there is an interseasonal storage system that would be able to capture a sufficient amount of freshness during the cool season.

Then, the analysis of the building performance indicators leads to several conclusions. First, the building with no insulation and low thermal inertia exploits more cooling energy from external convection and from the sky vault, but that is clearly at the expense of a great amount of heat passing through the envelope. This solution is not reasonable since it leads to higher air-conditioning demand.

The other building configurations mostly exploit the ventilation cooling resource. An intelligent way of controlling the airflow through the building would offer a great opportunity to decrease the air conditioning cooling needs. However, this would be valuable only during the cool season. For the same buildings, the external convection and sky exploitation potentials are generally low. Those low values reveal the limit of passive envelopes for the exploitation of those resources. Then, a building designer could consider active systems to collect freshness from the sky vault only when it is available.

Finally, it is worth mentioning the different orders of magnitude between the external and internal energy potentials and the predominance of the solar radiation on the external

heat loads. Sun shades are clearly a good option for decreasing the cooling needs in buildings.

6. Conclusion and outlook

In the present paper, the authors defined two sets of bioclimatic indicators, one for the quantification of the amount of cooling (heating) energy of a given resource that could be exploited (sheltered) and the other for the assessment of these resources (heat sources) exploitation (sheltering) by the building. These indicators are adapted to air-conditioned buildings in hot and humid climates. The sets of indicators were confronted with a basic test case. This confrontation showed that the information that can be drawn from the analysis of the indicators is valuable. They can orientate the choice of architects toward pertinent solutions in terms of bioclimatic architecture. The computation of the present indicators does not intend to replace the tools that are already used under the scope of bioclimatic procedures, such as shading maps or bioclimatic charts. They just intend to enrich the procedures by providing an overview of the exploitable resource and of the capacity of the building to exploit those resources.

The list of indicators that are defined in the present paper is not exhaustive. Since the motivation behind the development of those indicators was to assess the possibility of exploiting bioclimatic resources in a hot and humid climate, the soil was not considered a potential resource because of its high temperature. For different locations, it would be valuable to consider this resource.

Moreover, the test case revealed the limitation of passive envelopes in their ability to exploit external resources such as the sky vault. For such environmental resources, active systems such as sky radiant cooling would be helpful.

This new set of indicators can be easily adopted by designers and architects looking for optimal bioclimatic solutions in the early stages of building design. It could also be devoted to decision-making for the development of energy policies to spread the use of passive cooling solutions to reduce the building's cooling consumption.

Acknowledgements

The authors would like to thank the 'Agence Universitaire de la Francophonie, the University of Djibouti and the Center for Energy and Thermal Sciences of Lyon for providing facilities for research and for the funding of this project.

References

[1] R. Missaoui, Elaboration d'une stratégie et d'un plan d'action de maîtrise de l'énergie à Djibouti, Ministère de l'Energie en charge des Ressources Naturelles, Djibouti, 2015.

[2] M. Kottek, J. Grieser, C. Beck, B. Rudolf, F. Rubel, World Map of the Köppen-Geiger climate classification updated, Meteorologische Zeitschrift. (2006) 259–263. https://doi.org/10.1127/0941-2948/2006/0130.

[3] F. Butera, R. Adhikari, N. Aste, Sustainable Building Design for Tropical Climates: Principles and Applications for Eastern Africa, UN-Habitat, 2014.

[4] I.R. Edmonds, P.J. Greenup, Daylighting in the tropics, Solar Energy. 73 (2002) 111–121. https://doi.org/10.1016/S0038-092X(02)00039-7.

[5] A.A. Freewan, L. Shao, S. Riffat, Optimizing performance of the lightshelf by modifying ceiling geometry in highly luminous climates, Solar Energy. 82 (2008) 343–353. https://doi.org/10.1016/j.solener.2007.08.003.

[6] E. Mazria, The passive solar energy book, Rodale Press, 1979.

[7] B. Givoni, Impact of planted areas on urban environmental quality: A review, Atmospheric Environment. Part B. Urban Atmosphere. 25 (1991) 289–299. https://doi.org/10.1016/0957-1272(91)90001-U.

[8] K. Liu, B. Baskaran, Thermal performance of green roofs through field evaluation, Proceedings for the First North American Green Roof Infrastructure Conference, Awards, and Trade Show. (2003).

[9] C. Yu, W.N. Hien, Thermal benefits of city parks, Energy and Buildings. 38 (2006) 105–120. https://doi.org/10.1016/j.enbuild.2005.04.003.

[10] I.R. Edmonds, Performance of laser cut light deflecting panels in daylighting applications, Solar Energy Materials and Solar Cells. 29 (1993) 1–26. https://doi.org/10.1016/0927-0248(93)90088-K.

[11] M. Köhl, G. Jorgensen, S. Brunold, B. Carlsson, M. Heck, K. Möller, Durability of polymeric glazing materials for solar applications, Solar Energy. 79 (2005) 618–623. https://doi.org/10.1016/j.solener.2005.04.011.

[12] W. Lorenz, A glazing unit for solar control, daylighting and energy conservation, Solar Energy. 70 (2001) 109–130. https://doi.org/10.1016/S0038-092X(00)00132-8.

[13] J. Reppel, I.R. Edmonds, Angle-selective glazing for radiant heat control in buildings: theory, Solar Energy. 62 (1998) 245–253. https://doi.org/10.1016/S0038-092X(98)00006-1.

[14] G.B. Smith, S. Dligatch, F. Jahan, Angular selective thin film glazing, Renewable Energy. 15 (1998) 183–188. https://doi.org/10.1016/S0960-1481(98)00151-7.

[15] C.G. Granqvist, S. Green, G.A. Niklasson, N.R. Mlyuka, S. von Kræmer, P. Georén, Advances in chromogenic materials and devices, Thin Solid Films. 518 (2010) 3046–3053. https://doi.org/10.1016/j.tsf.2009.08.058.

[16] A. Synnefa, M. Santamouris, H. Akbari, Estimating the effect of using cool coatings on energy loads and thermal comfort in residential buildings in various climatic conditions, Energy and Buildings. 39 (2007) 1167–1174. https://doi.org/10.1016/j.enbuild.2007.01.004.

[17] M. Museli, Passive cooling for air-conditioning energy savings with new radiative low-cost coatings, Energy and Buildings. 42 (2010) 945–954. https://doi.org/10.1016/j.enbuild.2010.01.006.

[18] E. Bozonnet, M. Doya, F. Allard, Cool roofs impact on building thermal response: A French case study, Energy and Buildings. 43 (2011) 3006–3012. https://doi.org/10.1016/j.enbuild.2011.07.017.

[19] G. Baldinelli, Double skin façades for warm climate regions: Analysis of a solution with an integrated movable shading system, Building and Environment. 44 (2009) 1107–1118. https://doi.org/10.1016/j.buildenv.2008.08.005.

[20] M. Ciampi, F. Leccese, G. Tuoni, Ventilated facades energy performance in summer cooling of buildings, Solar Energy. 75 (2003) 491–502. https://doi.org/10.1016/j.solener.2003.09.010.

[21] N. Hamza, Double versus single skin facades in hot arid areas, Energy and Buildings. 40 (2008) 240–248. https://doi.org/10.1016/j.enbuild.2007.02.025.

[22] A.I. Omar, J. Virgone, E. Vergnault, D. David, A.I. Idriss, Energy Saving Potential with a Double-Skin Roof Ventilated by Natural Convection in Djibouti, Energy Procedia. 140 (2017) 361–373. https://doi.org/10.1016/j.egypro.2017.11.149.

[23] J.L. Molina, E. Erell, S. Yannas, Roof Cooling Techniques: A Design Handbook, Routledge, 2013.

[24] S. Raeissi, M. Taheri, Skytherm: an approach to year-round thermal energy sufficient houses, Renewable Energy. 19 (2000) 527–543. https://doi.org/10.1016/S0960-1481(99)00079-8.

[25] S.N. Kharrufa, Y. Adil, Roof pond cooling of buildings in hot arid climates, Building and Environment. 43 (2008) 82–89. https://doi.org/10.1016/j.buildenv.2006.11.034.

[26] B. Givoni, Passive Low Energy Cooling of Buildings, John Wiley & Sons, 1994.

[27] M. Santamouris, D. Asimakopoulos, Passive Cooling of Buildings, James & James, 1996.

[28] N.A. M. Al-Tamimi, S.F. Syed Fadzil, W.M. Wan Harun, The Effects of Orientation, Ventilation, and Varied WWR on the Thermal Performance of Residential Rooms in the Tropics, Journal of Sustainable Development. 4 (2011). https://doi.org/10.5539/jsd.v4n2p142.

[29] O. Saadatian, L.C. Haw, K. Sopian, M.Y. Sulaiman, Review of windcatcher technologies, Renewable and Sustainable Energy Reviews. 16 (2012) 1477–1495. https://doi.org/10.1016/j.rser.2011.11.037.

[30] A. Aflaki, N. Mahyuddin, Z. Al-Cheikh Mahmoud, M.R. Baharum, A review on natural ventilation applications through building façade components and ventilation openings in tropical climates, Energy and Buildings. 101 (2015) 153–162. https://doi.org/10.1016/j.enbuild.2015.04.033.

[31] G. Elshafei, A. Negm, M. Bady, M. Suzuki, M.G. Ibrahim, Numerical and experimental investigations of the impacts of window parameters on indoor natural ventilation in a residential building, Energy and Buildings. 141 (2017) 321–332. https://doi.org/10.1016/j.enbuild.2017.02.055.

[32] M. Benhammou, B. Draoui, Simulation et caractérisation d'un échangeur géothermique à air destiné au rafraîchissement des bâtiments fonctionnant dans les conditions climatiques du sud de l'Algérie, http://www.webreview.dz. (2015). http://www.webreview.dz/spip.php?article2365 (accessed March 1, 2018).

[33] B Draoui, Mebarki B, Abdessemed S, Keboucha A, Drici S, Sahli A, Etude d'un système de climatisation intégrant un puits canadien dans les zones arides, cas de Béchar, cder. (2015).

[34] H. NEBBAR, O. HAMDI, N. MOUMMI, A. BRIMA, Etude de comportement thermique d un échangeur enterré air/sol Expérimentation de Biskra (Algérie), (2014). http://docplayer.fr/37994327-Etude-de-comportement-thermique-d-un-echangeur-enterre-air-sol-experimentation-de-biskra-algerie.html (accessed June 19, 2018).

[35] B. Givoni, Comfort, climate analysis and building design guidelines, Energy and Buildings. 18 (1992) 11–23. https://doi.org/10.1016/0378-7788(92)90047-K.

[36] L. Pajek, M. Košir, Can building energy performance be predicted by a bioclimatic potential analysis? Case study of the Alpine-Adriatic region, Energy and Buildings. 139 (2017) 160–173. https://doi.org/10.1016/j.enbuild.2017.01.035.

[37] S. Semahi, N. Zemmouri, M.K. Singh, S. Attia, Comparative bioclimatic approach for comfort and passive heating and cooling strategies in Algeria, Building and Environment. 161 (2019) 106271. https://doi.org/10.1016/j.buildenv.2019.106271.

[38] L. Guan, M. Bennett, J. Bell, Evaluating the potential use of direct evaporative cooling in Australia, Energy and Buildings. 108 (2015) 185–194. https://doi.org/10.1016/j.enbuild.2015.09.020.

[39] N.A. Al-Azri, Development of a typical meteorological year based on dry bulb temperature and dew point for passive cooling applications, Energy for Sustainable Development. 33 (2016) 61–74. https://doi.org/10.1016/j.esd.2016.05.001.

[40] M. S. V. Szokolay PhD. MArch DipArch.FRAIA. RIBA, Climate analysis based on the psychrometric chart, International Journal of Ambient Energy. 7 (1986) 171–182. https://doi.org/10.1080/01430750.1986.9675499.

[41] C. Ghiaus, F. Allard, Potential for free-cooling by ventilation, Solar Energy. 80 (2006) 402–413. https://doi.org/10.1016/j.solener.2005.05.019.

[42] N. Artmann, H. Manz, P. Heiselberg, Climatic potential for passive cooling of buildings by night-time ventilation in Europe, Applied Energy. 84 (2007) 187–201. https://doi.org/10.1016/j.apenergy.2006.05.004.

[43] C.-A. Roulet, M. Germano, F. Allard, C. Ghiaus, Potential for natural ventilation in urban context: an assessment method, Indoor Air. (2002) 6.

[44] Y. Chen, Z. Tong, A. Malkawi, Investigating natural ventilation potentials across the globe: Regional and climatic variations, Building and Environment. 122 (2017) 386–396. https://doi.org/10.1016/j.buildenv.2017.06.026.

[45] M. Kaboré, E. Bozonnet, P. Salagnac, M. Abadie, Indexes for passive building design in urban context – indoor and outdoor cooling potentials, Energy and Buildings. 173 (2018) 315–325. https://doi.org/10.1016/j.enbuild.2018.05.043.

[46] G. Chiesa, Calculating the geo-climatic potential of different low-energy cooling techniques, Build. Simul. 12 (2019) 157–168. https://doi.org/10.1007/s12273-018-0481-5.

[47] F. Flourentzou, J. Van der Maas, C.-A. Roulet, Natural ventilation for passive cooling: measurement of discharge coefficients, Energy and Buildings. 27 (1998) 283–292. https://doi.org/10.1016/S0378-7788(97)00043-1.

[48] P. Chandra, Rating of wall and roof sections—Thermal considerations, Building and Environment. 15 (1980) 245–251. https://doi.org/10.1016/0360-1323(80)90006-2.

[49] C. Kabre, A new thermal performance index for dwelling roofs in the warm humid tropics, Building and Environment. 45 (2010) 727–738. https://doi.org/10.1016/j.buildenv.2009.08.017.

[50] G. Barrios, G. Huelsz, J. Rojas, J.M. Ochoa, I. Marincic, Envelope wall/roof thermal performance parameters for non air-conditioned buildings, Energy and Buildings. 50 (2012) 120–127. https://doi.org/10.1016/j.enbuild.2012.03.030.

[51] A. Muscio, H. Akbari, An index for the overall performance of opaque building elements subjected to solar radiation, Energy and Buildings. 157 (2017) 184–194. https://doi.org/10.1016/j.enbuild.2017.01.010.

[52] L. Chesné, T. Duforestel, J.-J. Roux, G. Rusaouën, Energy saving and environmental resources potentials: Toward new methods of building design, Building and Environment. 58 (2012) 199–207. https://doi.org/10.1016/j.buildenv.2012.07.013.

[53] ANSI/ASHRAE/IES Standard 90.1-2016 Energy Standard for Buildings Except Low-Rise Residential Buildings (I-P Edition) – Illuminating Engineering Society, (n.d.). https://www.ies.org/product/ansi-ashrae-ies-standard-90-1-2016-energy-standard-for-buildings-except-low-rise-residential-buildings-i-p-edition/ (accessed March 17, 2019).

[54] M.N. Inanici, F.N. Demirbilek, Thermal performance optimization of building aspect ratio and south window size in five cities having different climatic characteristics of Turkey, Building and Environment. 35 (2000) 41–52. https://doi.org/10.1016/S0360-1323(99)00002-5.

[55] W.H. McAdams, Heat transmission, McGraw-Hill, New York, 1954.

[56] K. Hiyama, L. Glicksman, Preliminary design method for naturally ventilated buildings using target air change rate and natural ventilation potential maps in the United States, Energy. 89 (2015) 655–666. https://doi.org/10.1016/j.energy.2015.06.026.

[57] J. Axley, Application of Natural Ventilation for U.S. Commercial Buildings Climate Suitability Design Strategies & Methods Modeling Studies, (2018).

[58] M. Centeno, New formulae for the equivalent night sky emissivity, Solar Energy. 28 (1982) 489–498. https://doi.org/10.1016/0038-092X(82)90320-6.

[59] E. Clarck, C. Allen, The estimation of atmospheric radiation for clear and cloudy skies, Proceedings of the Second National Passive Solar Conference. 2 (1978) 675–678.

[60] D. Dunham, Building for the maritime desert: climate, construction, and energy in Djibouti, Volunteers in Technical Assistance, Arlington, Va. (1815 N. Lynn St., Suite 200, Arlington 22209), 1983.